České vysoké učení technické v Praze
Fakulta elektrotechnická

Czech Technical University in Prague
Faculty of Electrical Engineering

Ing. Milan Polívka, Ph.D.

Extrémně nízkoprofilové antény pro rádiovou identifikaci (RFID) osob v pásmu UHF

Extremely low-profile antennas for radiofrequency identification (RFID) of people in UHF band

Summary

The lecture is devoted to the problems of low-profile antennas of data transponders of the radiofrequency identification (RFID) systems operating in UHF band designed for identification of people. Novel techniques for achievement of a very low antenna profile and maintenance of sufficient radiation efficiency are described as well as possibilities of tuning their complex input impedance. Proposed identification transponders have been tested for read range and identification reliability with the help of real RFID systems in indoor and open areas. We also solved the issues of optimal setting of the used systems for maximization of power margin in the area of identification, predominantly the influence of pointing and the shape of radiation pattern of reader antennas, interferences of reflected signals, shadowing the signal by other person. Mathematical modeling and computer simulation has been performed before the real testing and proved a good agreement with them. RFID system tuned for tested application (identification of sportsmen) validated reliability of identification and practical applicability of the proposed concepts.

Souhrn

Přednáška se věnuje problematice nízkoprofilových antén datových nosičů (tagů, transpondérů) pro systémy rádiové identifikace (RFID) pracující v pásmu UHF určené pro identifikaci osob příp. kovových objektů. Popisuje nové techniky dosažení velmi nízkého profilu při zachování dostatečné vyzařovací účinnosti a možnosti ladění komplexní vstupní impedance antén. Navržené nosiče byly testovány na čtecí dosah a spolehlivost identifikace s reálnými RFID systémy v interiérech i otevřených prostorech. Řešeny byly i aspekty optimálního nastavení použitého identifikačního systému maximalizující výkonovou rezervu v oblasti čtení, především vlivy směrování a tvaru vyzařovacích diagramů čtecích antén, interference odražených signálů či zastínění jinou osobou. Praktickým měřením předcházela tvorba matematických modelů a počítačových simulací, s nimiž prokázala dobrou shodu. RFID systém vyladěný pro testovanou aplikaci (identifikaci sportovců) osvědčil spolehlivost identifikace a praktickou použitelnost navržených konceptů.

Klíčová slova: datový nosič, dipól, nízkoprofilová anténa, monopól, víceprvkový dipól, patch, radiová identifikace

Keywords: data transponder, dipole, low-profile antenna, monopole, multiple element dipole, patch, radiofrequency identification

Contents

Introduction

One of the challenges within the application of passive radiofrequency identification (RFID) systems which is not treated satisfactory yet is reliable identification of people in indoor and open areas at the distances of a few or in optimal case even more than ten meters. Such distant identification might be enabled with the use of RFID systems operating in ultra-high frequency (UHF) band (860 – 960 MHz) due to the coupling between the reader and the transponder via propagation of electromagnetic wave. Other commonly used RFID systems operating in low-frequency (LF, 125 kHz), and high-frequency (HF, 13.56 MHz) bands are not suitable due to the very low radiated power as the size of coupling device (coil) is typically three or four orders of magnitude lower than the used wavelength, and consequently the read range is small, typically up to few decimeters.

A typical passive RFID system for UHF band consists of a transmitter/receiver (TX/RX) sometimes called reader, TX/RX antennas and a set of low cost data transponders or tags (integrated circuit called chip connected to a small thin antenna) placed on objects to be identified [1]. Such system often operates on a principle of backscattering, i.e. reader transmits a continuous electromagnetic wave which is reflected back by a tag which varies its reflection coefficient based on the unique identification number encoded in a chip supplied from energy of incident wave.

The received signal strength (RSS) which have to be higher than the sensitivity of the chip of the data transponder in the reading area is determined by Friis formula i.e. radio-communication equation. It comprises the transmitted power, gain of the TX/RX reader and transponder antennas, propagation free space losses, and additional kind of losses typically attributed to fast fading due to the interferences of direct and reflected signals. Some of the parameters of the equation are done by the used technology or legislation, e.g. maximum transmitted power. Another parameter such as propagation losses are determined by the physical laws and may vary in the certain range with the signal interferences. In general, more problems are associated with the transponder antennas as it will be described later on. Insufficient performance of transponder antenna parameters can thus substantially impact on the power budgets and result in an erroneous or even no identification. Efficient and reliable identification of people is thus a relatively difficult technical task.

The following text focuses first on the design of novel concepts, and performance evaluation of very low-profile radiators able to efficiently operate closely spaced to the human body. Further, we present a set of read range tests and evaluation of identification reliability of real passive RFID systems operating in UHF band [2], [3]. We solved the issues of optimal setting of the used system for maximization of power margin in the area of identification, predominantly the influence of pointing and the shape of radiation pattern of reader antennas, interferences of reflected signals, shadowing the signal by other person. Mathematical modeling and computer simulation has been performed before the performance evaluation and testing and proved a good agreement. Optimized RFID system has confirmed a reliability of identification and practical applicability of the proposed concepts.

1 Wearable low-profile tag antennas for radiofrequency identification of people

The design of UHF transponder antennas suitable for identification of people has several important requirements, some of them being slightly different from demands on standard communication antennas:

- Immunity of antenna parameters from the nearby presence of a human body,
- Impedance matching to the complex impedance of the chip,
- Low profile, small footprint dimensions, and low weight; eventually also flexibility.

One of the problems that must be solved considering the identification of people in UHF band is the degradation of the TAG antenna performance in the close vicinity of a human body. The body can be treated as a high-loss dielectric object with a relative permittivity $\varepsilon_r \sim 50 - 60$ and loss tangent $\tan\delta \sim 0.5 - 1.2$ [4]. In case of the standard dipole type TAG antennas, the presence of such dielectric objects causes significant detuning of the antenna and absorption of the radiated or received energy [5] - [8]. This results in a low radiation efficiency and consequently in a short read distance. The problem of frequency detuning and energy absorption can be, in principle, solved by insertion of distant spacer which, on the other hand, increases the vertical profile. Another solution is an insertion of a metallic plate between radiator and body that acts as a screening plane or is an inherent part of the antenna structure. The former solution might be used in a case of dipole or loop-type antennas [6], [7], while patch and PIFA antennas [9] - [12] usually represent the latter case.

Electrical performance requirement on the wearable transponder antennas for the UHF band is conjugate matching to the complex input impedance of the chip which is typically capacitive. Small dimensions, very low profile and low weight; eventually flexibility are physical requirements for the convenience of the persons carrying the transponder.

Thus, the challenge in the research of UHF transponder antennas is a development of radiators of very low vertical height over a shielding conductive plane (typically bellow $0.01\lambda_0$, i.e. smaller than approx. 3 mm) concurrently with the maintenance of a sufficient radiation and antenna efficiency.

The following two subchapters first concerns the problems of low radiation efficiency in case of standard dipole-type antennas placed closely above the metallic plane and patch-type antennas with relative height of the substrate smaller then approx. $0.01\lambda_0$. Original very low-profile solutions using multiple-element dipole, and the novel dual-element shorted-patch antennas for maintenance of sufficient radiation efficiency and tuning capability for required complex input impedance are presented. All these solutions exhibit polarization of radiated electromagnetic wave parallel with the screening plane.

1.1 Dipole-type antennas

As mentioned above the dipole-type antennas closely spaced above conductive shielding screen; see Fig. 1a suffer from low radiation efficiency that may be explained simply by application of the image principle. Image current denoted I_2 below the conductive plane have the opposite direction in face of the source dipole current I_1. Dipole input impedance can be expressed as $Z_{in} = Z_{11} + I_2/I_1 Z_{12}$; where Z_{11} is a self-impedance of the dipole, Z_{12} is the mutual impedance of the dipole and its image. Current magnitudes may be considered nearly the same ($I_2 \approx -I_1$) for small distances of source and image currents ($h/\lambda_0 << 1/20$). For $h/\lambda_0 \to 0$ self and mutual impedances are comparable $Z_{11} \sim Z_{12}$, consequently $Z_{in} \to 0$ and dominant real part of the input impedance (radiation resistance) $R_{rad} \to 0$ as well. As a result, the radiation and antenna (1) efficiencies significantly decrease for $h/\lambda_0 \to 0$; see Fig. 1c, d.

$$\eta_{rad} = \frac{R_{rad}}{R_{rad} + R_{loss}}, \quad \eta_{ant} = \eta_{rad} \cdot \left(1 - |\Gamma|\right) \tag{1}$$

R_{loss} is a loss resistance of the antenna which is typically very small for good conductors, and Γ is a reflection coefficient at the input port.

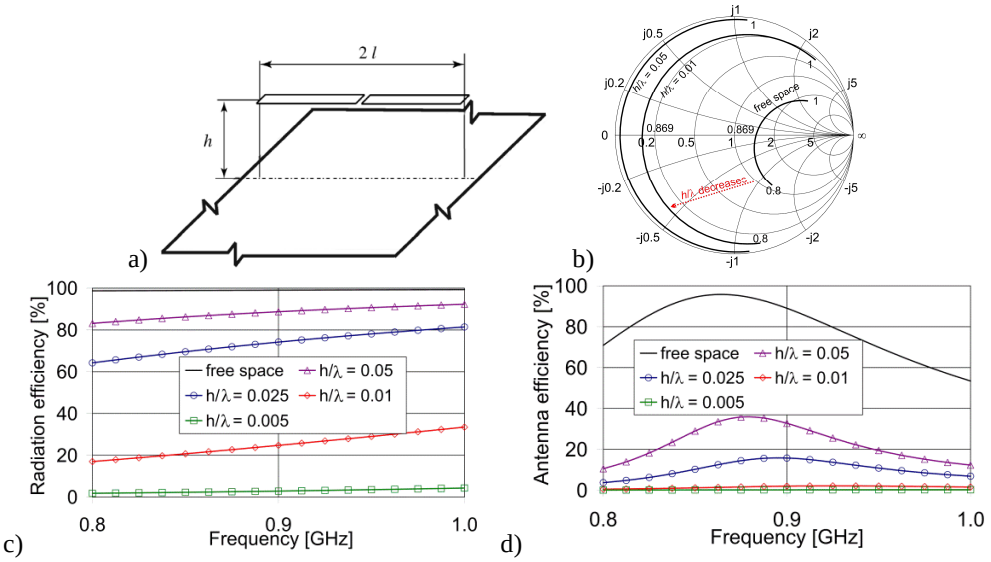

Fig. 1 Simulation of a half-wave planar dipole placed above an infinite conductive plane, for details see [13]: a) sketch of the arrangement, b) input impedance curves in the Smith chart as a function of relative dipole distance over the conductive plane, c), and d) radiation and antenna efficiencies (method of moment simulator IE3D).

1.1.1 Multi-element folded dipoles

One of the possible solutions that raise the radiation resistance of a dipole-type antennas operating above the close conductive plane is the application of multi-element folded dipoles. These structures may provide an extremely low profile (even below the relative height 0.01 λ_0) and, at the same time, maintain the sufficient radiation efficiency (over 50 %). Nevertheless, the relatively large footprint dimensions comparable with the half-wavelength might be limiting factor for certain RFID applications.

Based on our previous work on multi-element folded dipoles [13] we proposed, designed, and measured 5-element folded dipole placed on two-layer substrate composed of 2.4 mm thin foam substrate and 0.09 mm thin GML 1100 woven-glass laminate backed by a conducting plate [14]. The folded dipole length is 155 mm, the width is 14 mm, spacing of elements is 0.8 mm, strips width is 2.2 mm. The total antenna size including shielding metallic plate is 180 × 36 × 2.5 mm (0.52 × 0.1 × 0.007 λ_0@869 MHz). The central element has been fed by a chip of the impedance Z_{chip} = 22 - j195 Ω. The real part of complex conjugate antenna impedance has been achieved by appropriate number of elements and imaginary part by proper tuning of the length over the half wavelength resonance; see Fig. 2b. The measured antenna efficiency and gain of this design was between 40 - 50 % (irrespective of whether it is placed in free space or enclosed to human body phantom) and 1.3 dBi, respectively.

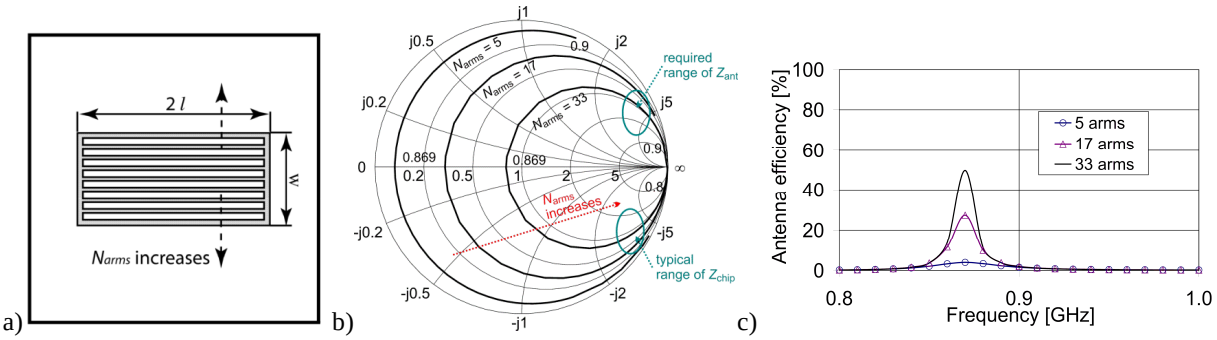

Fig. 2 *N*-element folded dipole placed closely (*h* = 1.04 mm; ~ 0.003λ_0 @869 MHz) over a perfect conducting plane, a) sketch, b) curves of input impedance in a Smith chart, c) simulated antenna efficiency; details in [13].

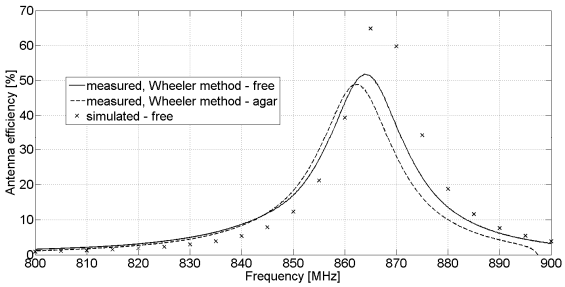

a) b)

Fig. 3 The 5-element folded dipole placed on the foam dielectric shielded by a metallic screen: a) sketch, b) curves of input impedance in a Smith chart, c) photograph of a manufactured sample, d) its antenna efficiency.

1.2 Patch-type antennas

The employment of the patch-type and PIFA antennas, where a metallic ground plane is an inherent part of the antenna structure, represents another possible concept for very low-profile antennas. But, it is necessary to take into account the fundamental fact that their radiation efficiency decreases significantly [15], when substrate height is lower than approx. 0.01 - 0.02 λ_0 (3.5 – 6 mm); see Fig. 4. For wearable UHF TAG antennas, such height might be limiting in a certain radiofrequency identification applications.

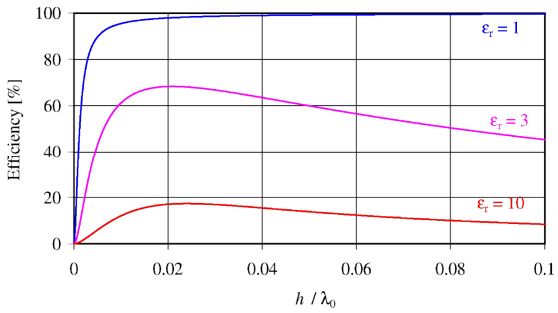

Fig. 4 Radiation efficiency of a patch antenna as a function of relative substrate height, calculated according to [15]

1.2.1 Foam substrate patch antenna

A patch antenna [2] for identification of sportsmen, see Fig. 5, was proposed and fabricated on a foam dielectric (G3 9568 foam h = 4.8 mm, $h/\lambda_0 \sim 0.014$) using a conductive fabric. The weight of the antenna is approx. equal to 20 g, it is flexible and, it is intended to be easily integrated into the sportsmens' number labels. The ground plane dimensions are 165 × 74 mm, the measured gain of an antenna placed on a human body is 5.0 dBi.

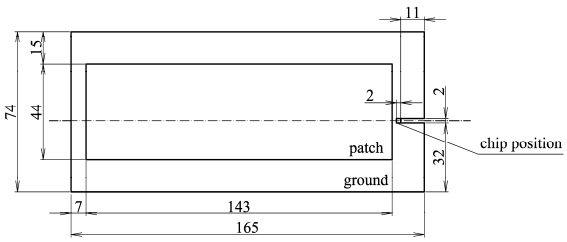

a) b)

Fig. 5. Patch TAG antenna: a) photograph, and b) sketch.

1.2.2 Small dual-loop antenna loaded by a patch array backed by grounded dielectric slab

Aimed at the development of a badge-sized chest-fixable TAG antenna, the electrically small flatten dual-loop antenna placed over a planar array of four sub-wavelength patches printed on a grounded

dielectric slab has been designed [16]. The footprint dual-loop size is 70 × 11 mm, the total size including the patch array printed on the grounded dielectric layer (1.58 mm, ε_r ~ 10) is 105 × 70 × 1.82 mm (relative size is 0.3 × 0.2 × 0.005 λ_0@869 MHz); see Fig. 6.

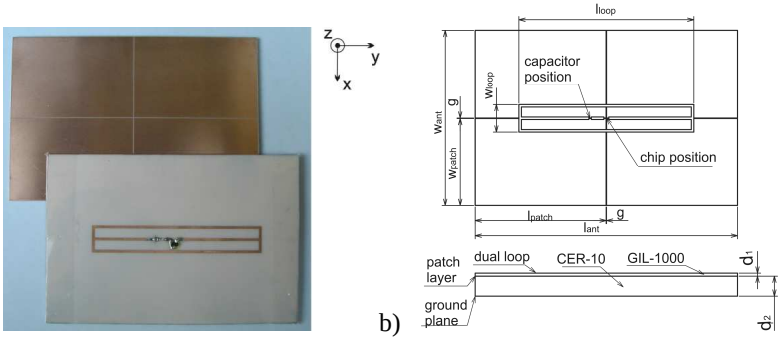

Fig. 6 Flat dual-loop antenna closely spaced over a metal-backed patch array with the substrate parameters d_1 = 0.24 mm, d_1/λ_0 ~ 0.0007, ε_{r1} ~ 3.05, d_2 = 1.58 mm, d_2/λ_0 ~ 0.0046, ε_{r2} ~ 10): a) photograph, b) sketch.

Comparison of radiation efficiency of the flat single-loop antenna in the free space, above the metallic plane, and above the four-element patch array and antenna efficiency of the antenna over patch array is demonstrated in Fig. 7. The only drawback is relatively high relative permittivity of the screening patch array substrate.

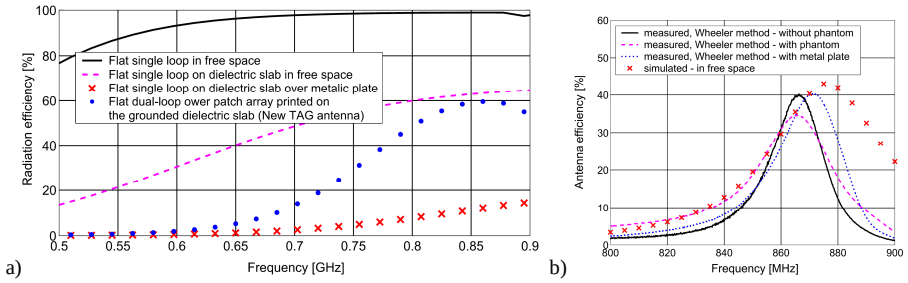

Fig. 7 Comparison of radiation and antenna efficiencies of the proposed dual-loop patch array antenna.

1.2.3 Slot-coupled dual-element shorted patches

The above-mentioned drawback of the dual-loop patch array antenna can be eliminated using a low permittivity substrate (ε_r = 3.2, tanδ = 0.002). However, this approach leads to a significantly larger patch array size, because the wavelength λ_g is equal to approx. 220 mm at frequency 869 MHz. The reduction of the screening four-element patches structure to the two-element structure is the first miniaturization step that does not result in the decrease in the radiation efficiency. The patch array length can be further reduced by the realization of the patches acting as a quarter-wavelength resonators, whose outer edge is conductively connected with the screening metallic plane; see Fig 8 and [17].

A planar meanderly folded dipole etched on the superstrate layer is used as an excitation element, whose length is used in order to tune the input impedance so that it is the complex conjugate to the chip impedance value. The total size of the dual-layer antenna [17] equals 95 × 60 × 1 mm (relative size is equal to 0.28 × 0.17 × 0.003 λ_0@869 MHz). The dipole dimensions follow: *la* = 28.5 mm, *lb* = 23.5 mm and *wa* = 8 mm.

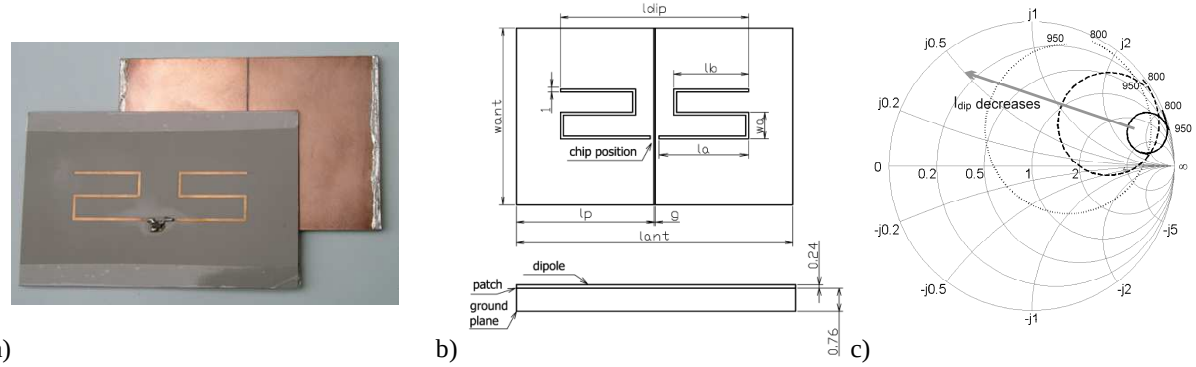

a) b) c)

Fig. 8 Coupled two-element shorted-patch excited by a folded dipole: a) photograph, b) sketch, and c) tuning of the impedance curve by change of the dipole length in a Smith chart.

The removal of the upper substrate represents another possibility how to simplify the structure of the antenna. The shorted two-element patch structure can be excited directly by the chip, inserted into the slot situated between the inner patch edges; see Fig. 9 and [17]. Unfortunately, this structure does not involve the capability of impedance tuning. By the insertion of two slots (as reactive elements that are, from both sides, symmetrically close to the inner slot), by setting of its distance, length and width the impedance matching can be achieved. The total size of the directly excited two-element shorted patch antenna is 100 × 60 × 0.76 mm (relative size is 0.29 × 0.17 × 0.0022 λ_0@869 MHz). The dimensions of the impedance slots follow: *ls* = 40 mm, *ws* = 6 mm and *p* = 3 mm. The antenna is, again, realized on the low-permittivity substrate ε_r = 3.2. Fig. 9c depicts the parametric dependence of the complex Z_{in} on the distance *p* (i.e. the distance between the impedance slot and the radiating slot). SMD capacitors act as a galvanic separation for used chip. It is evident that both, the magnitude and phase of Z_{in} can be easily tuned.

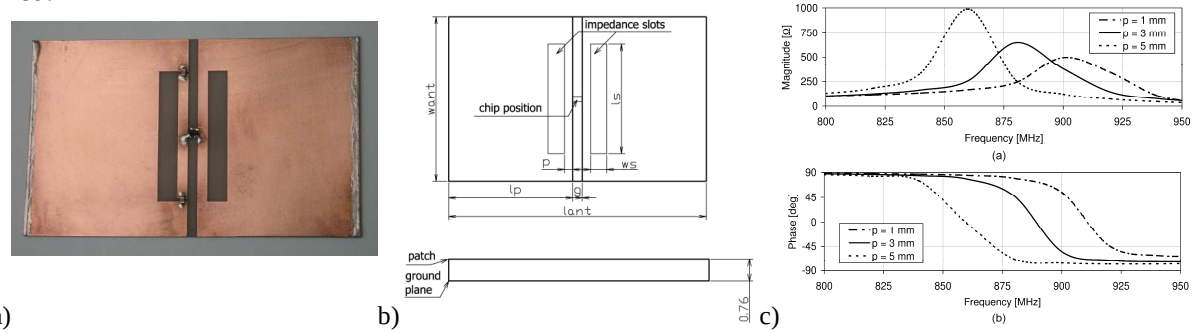

a) b) c)

Fig. 9 Coupled two-element shorted-patch with tuning slots with direct excitation: a) photograph, b) sketch, c) parametric dependence of magnitude and phase of antenna input impedance on the distance *p*.

The simulation and measurement of the antenna efficiencies of both antennas are depicted Fig. 10.

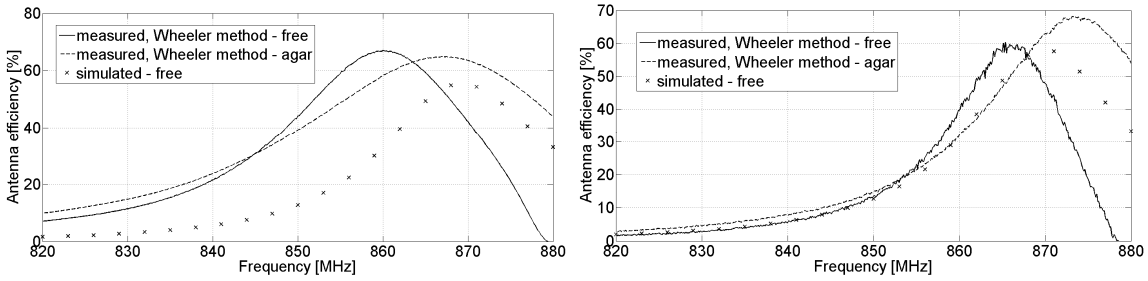

a) b)

Fig. 10 Antenna efficiencies of coupled dual-patch antennas a) dipole excited, b) directly excited with tuning slots

Performance properties of proposed antennas and comparison with selected commercially available antennas are summarized in Table 1; see also [3]. Note that proposed antennas yield the advantage of the design for narrow European UHF RFID band (865 – 869 MHz).

Antenna	Size (mm)	Relative size (λ_0)	ε_r (-)	m (g)	η_{ant} (%)	d_{max} (m)
Foam substrate patch	165 × 74 × 5.0	0.48 × 0.21 × **0.014**	~1.3	20	91[1)]/55[2)]	
5-arm dipole	180 × 36 × 2.5	0.52 × 0.1 × **0.007**	1.3	9	49[1)]/41[2)]	7.6
Dual-loop patch array	105 × 70 × 1.82	0.3 × 0.2 × **0.005**	10	38	33[1)]/39[2)]	4.8
Dipole excited	95 × 60 × 1.0	0.28 × 0.17 × **0.003**	3.2	14	47[1)]/64[2)]	3.9
Directly excited	100 × 60 × 0.76	0.29 × 0.17 × **0.002**	3.2	10	52[1)]/60[2)]	5.4
WF-SM-12	125 × 78.1 × 9.38	0.37 × 0.23 × 0.028		-		1.2
WF-SM-25	150 × 6.25 × 6.25	0.3 × 0.092 × 0.009		-		2.7
WF-SM-40	103 × 31.2 × 3.1	0.3 × 0.092 × 0.009		-		1.2
UHF metal tag-01	55 × 20 × 2.0	0.16 × 0.06 × 0.0059		-		3.0
UHF metal tag-06	150 × 18 × 2.0	0.44 × 0.053 × 0.0059		-		3.0

Tab. 1 Comparison of parameters and read distance (P_t = 1W, G_{reader} ~8 dBi) of proposed and selected commercially available TAG antennas for metallic surfaces operating in European UHF RFID band [3]. [1)] Free space, [2)] agar.

2 Optimization and performance evaluation of RFID system for identification of people

As it has been already mentioned, in order to identify people parameters of RFID system have to be optimized or tuned [2], [3]. The optimization should be particularly focused on:

- The selection of a suitable operating frequency and RFID system (reader, TAG chips). Low sensitivities $P_{rTAGmin}$ and $P_{rREADERmin}$ of TAG chip and reader are beneficial.
- The selection and implementation of a suitable propagation model, power budget calculations.
- The choice or design of suitable reader antennas, optimization of their positioning and tilt with respect to the identification area to maximize power margin.
- The choice or design of suitable TAG antennas. The most important features are immunity against the influence of the human body, small dimensions, low profile and weight.
- Evaluation of the propagation model and power margin by measurement, evaluation of possible random influences (shadowing, tilt), ensuring of required power margin.
- Practical identification tests of the tuned RFID system.

2.1 System parameters

A commercial RFID system operating in UHF band; see Table 2 and [18] were used for the evaluation of a read range in corridors and open areas and a reliability of identification of people.

System components	Parameter	Troley Ponder (chip Troley Ponder)
	Operating frequency	869 MHz
Reader	Transmitted power (dBm)	24.7 to 36.0
	Receiver sensitivity (dBm)	-64
	Reader antenna gain (dBi)	8.0
Transponder (TAG)	Chip sensitivity (dBm)	-6.9
	Chip impedance (meas.) (Ω)	76 - j340
	TAG conversion loss (dB)	20

Tab. 2 Parameters of UHF RFID system used

2.2 Propagation models and power budget

As mentioned already, the performance and reliability of the identification depend upon the reader-TAG and TAG-reader power budgets. The TAG chip input power P_{rTAG} must be higher that the chip sensitivity P_{rTAGmin}, and simultaneously the power P_{rREADER} at the input of the receiver must be higher than the reader sensitivity $P_{\mathrm{rREADERmin}}$

$$P_{\mathrm{rTAG}} \geq P_{\mathrm{rTAGmin}} \wedge P_{\mathrm{rREADER}} \geq P_{\mathrm{rREADERmin}} \tag{2}$$

The power P_{rTAG} in dBm can be expressed as

$$P_{\mathrm{rTAG}} = P_{\mathrm{t}} - L - L_{\mathrm{f}}\,, \tag{3}$$

where P_t is the RF power transmitted by the reader in dBm, L stands for the link loss and L_f represents the attenuation of the feeder cable in dB. The peak power of the modulated signal reflected back from the TAG and received by the reader receiver $P_{rREADER}$ in dBm can be expressed as

$$P_{\mathrm{rREADER}} = P_{\mathrm{rTAG}} - L - L_{\mathrm{f}} - L_{\mathrm{conv}}\,, \tag{4}$$

where L_{conv} is the conversion loss of the chip. The maximum read distance d_{max} can be defined as the longest distance d, where conditions (1) are simultaneously fulfilled. In order to evaluate the conditions of the identification in different environments, it is necessary to calculate the corresponding link loss L.

The propagation of an electromagnetic wave from the reader to the TAG in an open area can be described by the modified two-ray model, see Fig. 11a and [2]. The model takes two paths of electromagnetic waves between the reader and TAG into account; the first is formed by a direct ray, the second by a ray reflected from the ground. The resulting radio link loss can be evaluated by means of the following formula

$$L = -20\log\left(\left(\frac{\lambda}{4\pi}\right)\left|\sqrt{G_{\mathrm{tagV}}(\alpha_{\mathrm{d}})G_{\mathrm{rV}}(\beta_{\mathrm{d}})G_{\mathrm{tagH}}(\gamma)G_{\mathrm{rH}}(\delta)}\cdot\frac{1}{r_1}e^{-j\cdot k\cdot r_1} + \sqrt{G_{\mathrm{tagV}}(\alpha_{\mathrm{r}})G_{\mathrm{rV}}(\beta_{\mathrm{r}})G_{\mathrm{tagH}}(\gamma)G_{\mathrm{rH}}(\delta)}\cdot \mathrm{R}(\vartheta)\cdot\frac{1}{r_2}\cdot e^{-j\cdot k\cdot r_2}\right|\right) \tag{5}$$

where r_1, r_2 are the lengths of the direct and reflected rays, $G_{\mathrm{rV}}(\beta)$, $G_{\mathrm{rH}}(\delta)$ stand for approximated 3D angular dependencies of the reader antenna gain in the vertical and horizontal planes, $G_{\mathrm{tagV}}(\alpha)$, $G_{\mathrm{tagH}}(\gamma)$ represent angular dependencies of the TAG antenna gain in the vertical and horizontal planes, while $\overline{R}(\vartheta)$ is a complex reflection coefficient of the ground ($\varepsilon_{\mathrm{r}} = 10$, $\sigma = 10^{-2}$ S/m was considered).

The phenomena which influence reader-TAG link loss inside buildings are substantially more complicated compared to open areas. Since electromagnetic waves interact with many surrounding obstacles, multiple reflections and diffractions must be taken into account. Many models and methods can be found [19] - [21] which are applicable for calculating the path loss inside buildings.

In empirical models, approximate mathematical formulas are used to calculate the received power, which is proportional to the distance from the transmitter d by the term $(1/d)^n$, where n stands for the path-loss exponent which is affected by the geometry as well as the electrical properties of the given environment.

In open areas, the value of the path-loss exponent is close to $n = 2$, while in corridors, lower values are reported ($n = 1.4$ in [20]). That is why substantially longer read distances can be expected in corridors compared to open areas.

On the other hand, the deterministic or semi-deterministic models utilizing ray-tracing or ray launching methods [21] are based on the geometry of the particular task (see Fig. 11b) and can provide more precise results. In order to take into account as many propagation phenomena in corridors with the given dimensions and material parameters as possible, the 3D ray-tracing method implemented in the WinProp

program [22] was used. Up to six reflections and two diffractions (calculated by uniform theory of diffraction - UTD), from brick walls ($\varepsilon_r = 4$, $\sigma = 0.005$ S/m) and a concrete floor and ceiling ($\varepsilon_r = 6$, $\sigma = 0.003$ S/m) were considered.

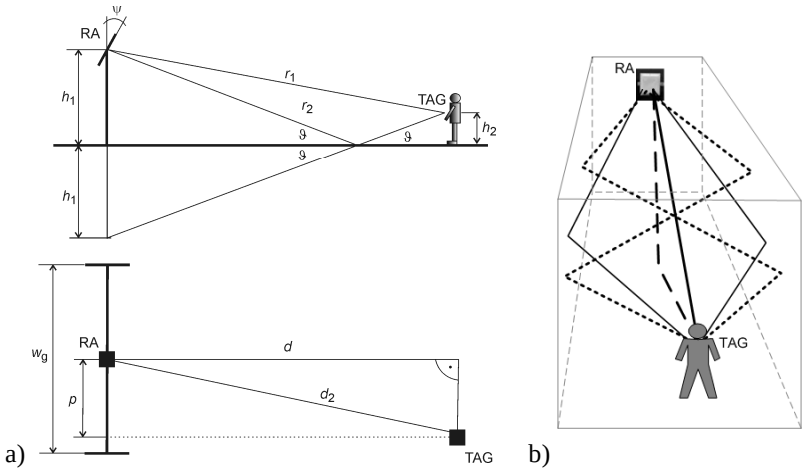

Fig.11 Configuration of a) a two-ray model: side-view (upper) top-view (bottom) with the following parameters: h_1 height of reader antenna, h_2 height of TAG antenna on person's chest, r_1 direct ray trace, r_2 reflected ray trace, d_2 ground plane distance between reader and TAG antennas, w_g width of identification area, p reader and TAG antenna axis offset, b) a six-ray model in a narrow corridor.

2.3 A novel gain enhanced reader antenna

In order to enhance the effective radiated power of the TX and RX reader antennas and to concentrate the energy at the expected identification area, a special collinear microstrip patch antenna with enhanced gain was proposed and developed [23]; see Fig. 12. It provides a wide radiation pattern in the horizontal plane and narrower pattern in the vertical plane with a corresponding higher gain (11.7 dBi compared to 8.0 dBi of the original reader antenna).

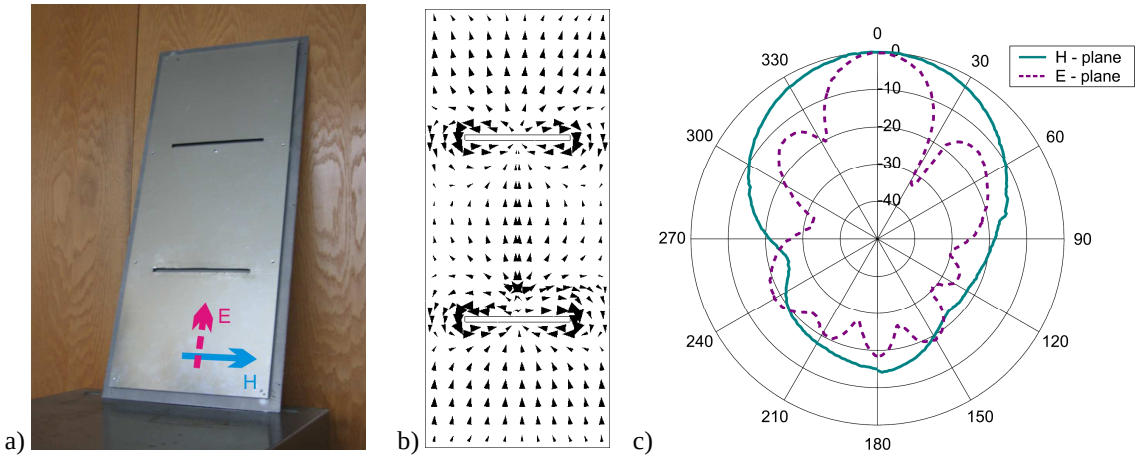

Fig. 12 A reader collinear microstrip patch antenna: a) photograph, b) vector surface current distribution, and c) measured radiation patterns.

2.4 Tuning of a tilt of the reader antennas

The simulation of the effect of a tilt of the reader antenna on the TAG input power P_{rTAG} is depicted in Fig. 13; see [2]. The plot indicates that the optimum tilt is $\psi = 30^o$. Higher tilt values result in a steep P_{rTAG} decline within the $3 \leq d \leq 4$ m range, whereas a lower ψ value provides a low TAG input power in

the vital region d < 4 m close to the gate, where a smaller influence of the shadowing of TAGs by neighboring sportsmen can be expected. The difference between the maximum receiver power on the axis (p = 0 m) and off the axis (p = 2.5 m) is about 4 dB. The ψ = 30º tilt was used for both other measurements and practical identification tests.

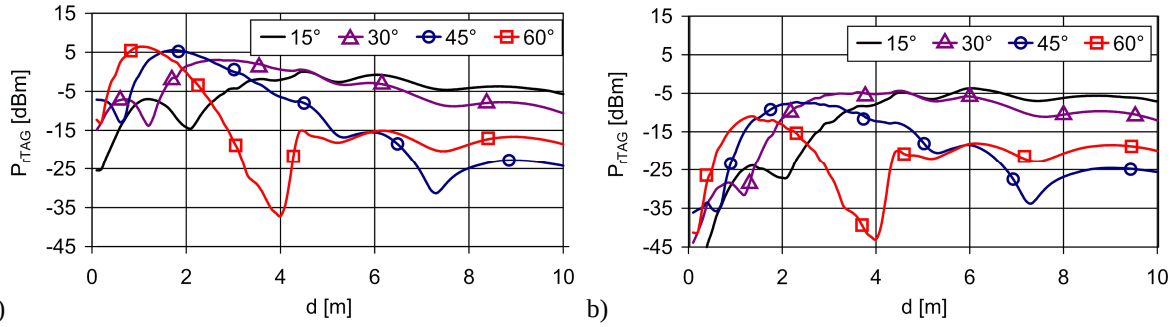

Fig. 13 Simulation of the TAG input power P_{rTAG} versus distance d for different tilt ψ of the reader antenna (P_t = 35.4 dBm, h_1 = 3 m, h_2 = 1.3 m) on the axis (p = 0 m) and off the axis (p = 2.5 m)

2.5 Influence of tilt of the TAG antenna

One possible additional loss can be caused by more or less random tilt of the TAG antenna caused by the natural tilt of a human body. It can be especially significant in the case of people running. These additional link losses were investigated by means of practical measurements. Fig. 14 shows the measured P_{rTAG} values as a function of the distance d from the gate (on the gate axis p = 0) and tilt φ of the person; see [2]. The presented data indicates that the tilt $\varphi > 0$ can result in significant additional loss, especially in the ranges $d \leq 2$ m and $d > 7$ m. Nevertheless, in both of these regions, the simulated and measured P_{rTAG} values are below the $P_{rTAGmin}$ value even for $\varphi = 0$ (an erected person), and the identification is unlikely to be performed here. And on the contrary, the proper identification can be expected in the $2 \leq d \leq 7$ m range, where the influence of the person's tilt φ is relatively small and the additional loss caused by the tilt usually does not exceed 3 dB.

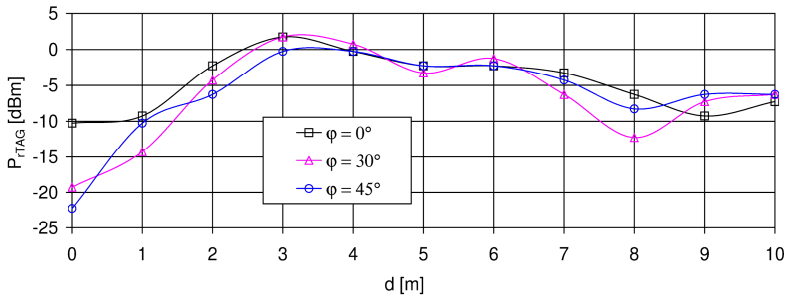

Fig. 14 Influence of tilt φ of a person on the received TAG power P_{rTAG} (measurement, P_t = 35.4 dBm, h_1 = 3 m, h_2 = 1.3 m, ψ = 30°, p = 0 m).

2.6 Influence of a person shadowing

If several people gather in a small area in an identification area, it may result in mutual shadowing and consequent additional path-loss. In practice, any configuration of people can appear. In order to get at least the basic information about this potential signal fading, a set of relatively simple measurements was performed. The P_{rTAG} values were measured at all positions but one person was always standing erectly at a distance of 1 m in front of a person wearing the measurement antenna. The results of these measurements are presented in Fig. 15 and [2]. As expected, the additional shadowing loss is strongly dependent on the distance d from the gate. Within the range $d \leq 3$ m, the influence of the shadowing is

negligible. In the range between $3 \le d \le 5$ m, this shadowing loss is up to 3 dB, for $d > 5$ m the shadowing loss is around 6 dB.

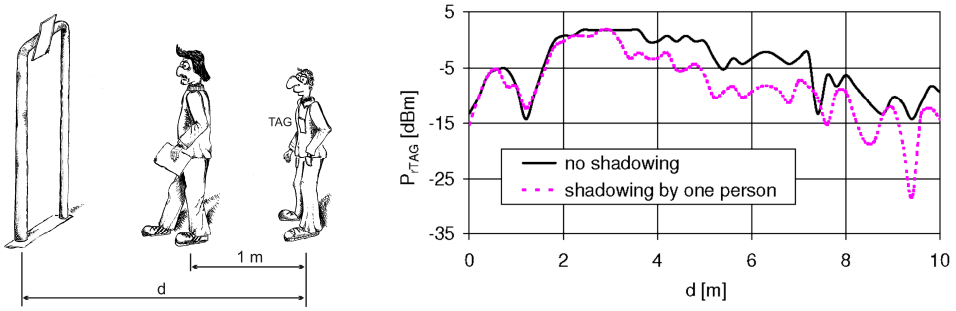

Fig. 15 Influence of shadowing on received signal strength (P_t = 35.4 dBm, h_1 = 3 m, h_2 = 1.3 m, ψ = 30°, p = 0 m)

2.7 Power budgets of the optimized RFID system

The following figures show the P_{rTAG} and $P_{rREADER}$ plots as a function of distance d from the gate and p from the gate axis [2]. To see the potential of the "tuning" procedure, the figures include the same dependencies measured with a meander dipole antenna fixed on a test person at a distance b = 20 mm without a screening metallic plate. Fig. 16 shows the plot of the simulated and measured TAG input power P_{rTAG} at the gate axis p = 0 m. Fig. 17 shows the simulated and measured P_{rTAG} values at the offset p = 2.5 m. Both figures include the corresponding $P_{rTAGmin}$ sensitivity value and compare the results obtained from the new RFID patch and the standard meander dipole. With the meander dipole antenna used, the P_{rTAG} values are above the $P_{rTAGmin}$ for p = 0 m, but with only 3 dB backup. For p = 2.5 m, P_{rTAG} is significantly below $P_{rTAGmin}$. That is why a non-optimized system can only work close to the gate axis and with low identification reliability. The optimized system show min. 6 dB backup even at the p = 2.5 m offset. That is why its identification reliability is 100 % in the entire required identification area and even under worst expected conditions; see Table 3.

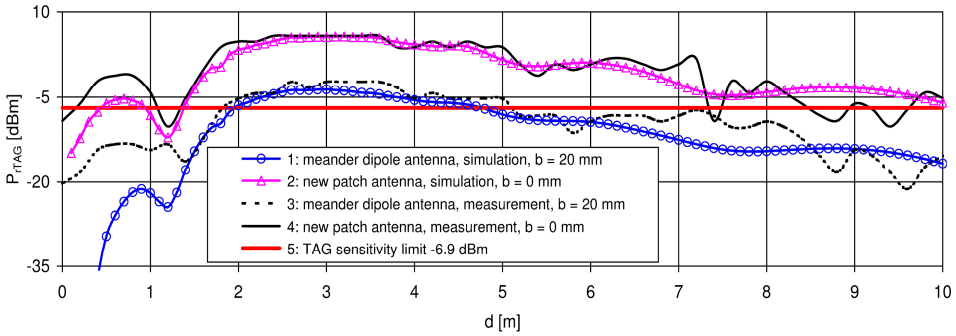

Fig. 16 Simulated and measured TAG input power P_{rTAG} on the reader-TAG trace (P_t = 35.4 dBm, h_1 = 3 m, h_2 = 1.3 m, ψ = 30°, p = 0 m)

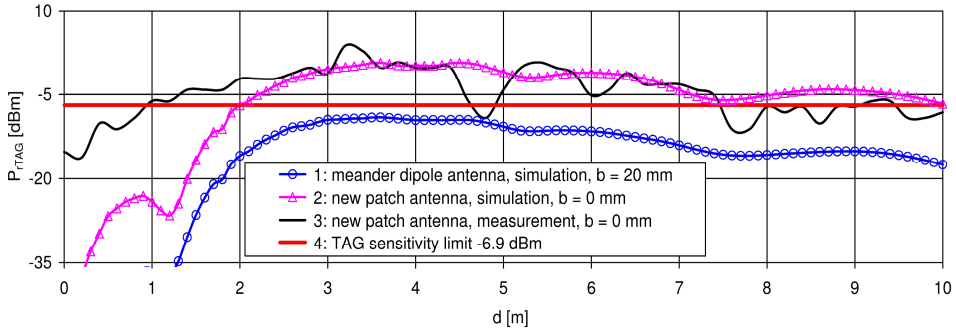

Fig. 17 Simulated and measured TAG input power P_{rTAG} on the reader-TAG trace (P_t = 35.4 dBm, h_1 = 3 m, h_2 = 1.3 m, ψ = 30°, p = 2.5 m)

Fig. 18 shows the simulated reader input power $P_{rREADER}$ values with respect to the reader sensitivity $P_{rREADERmin}$. Use of the standard meander dipole antenna leads to unacceptably low $P_{rREADER}$ values, especially off-axis. Employment of the RFID patch, optimized for operation on a human body, can guarantee high enough power even in this return TAG-reader link.

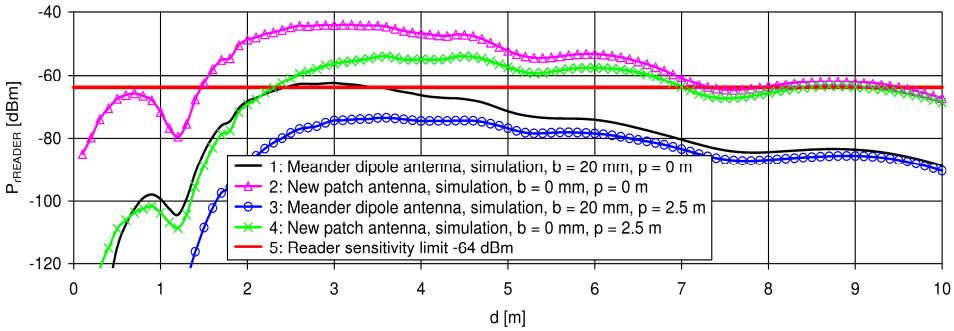

Fig. 18 Simulated input power $P_{rREADER}$ on the TAG-reader trace (P_t = 35.4 dBm, h_1 = 3 m, h_2 = 1.3 m, ψ = 30°).

2.8 Identification of sportsmen

In order to verify identification reliability of the optimized system, tests simulating real RFID system applications were performed [2]. A group of racers moved on an asphalt surface in several different formations, see Fig. 19. In the first formation, 7 racers moved in a row, in the second formation 7 racers formed a kind of a matrix. Each formation moved with 3 different speeds simulating a walk (approx. 4 km/h), a fast walk (approx. 8 km/h) and a run (approx. 15 km/h). Each test was repeated 3 times. For comparison, tests were performed using both the RFID patch and standard planar dipole TAG antennas fixed on thick foam spacer (b = 20 mm). The results of performed tests are presented in Table 4.

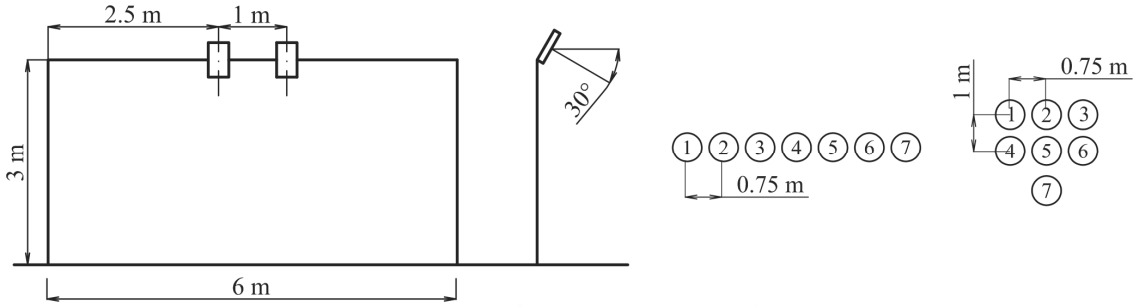

Fig. 19 Antenna gate dimensions a) and basic formations of racers used for testing of the optimized RFID system in b) row, c) matrix

Configuration of racers	Speed of racers	Percentage of correct identification (%)	
		Dipole	RFID patch
row	walk	66.7	100
	fast walk	52.4	100
	run	-	100
matrix p = 2.5 m	walk	61.7	100
	fast walk	52.4	100
	run	-	100
matrix p = 0 m	walk	85.7	100

Tab. 4. Reliability of identification of racers in open area obtained with dipole and the RFID patch TAG antennas.

2.9 Evaluation of received signal strength and read range in open and indoor areas

In order to verify and compare the performed simulations in open indoor area, the P_{rTAG} values were measured in several test configurations corresponding to typical scenarios in people identification tasks. Besides that, values of the maximum read distances d_{max} were also measured. The RF generator, the test antenna with the same gain as the new TAG antenna and a spectrum analyzer were used for P_{rTAG} measurements. The dual-loop patch array TAG antenna with the connected chip and reader were used for the d_{max} measurements. During both measurements, antennas were fixed on a person's chest in the height of 1.25 m, see Fig. 20.

Measurements were performed in narrow and wide corridors (width of 2 and 4 m, respectively) and in an open area in front of the building. The 4 m wide corridor has the following parameters: height of 3.35 m, length of 29 m, ended by a wall. The parameters of the 2 m wide corridor are: height of 3 m, length of 45 m, ended by a glass window. In all the configurations the standard 8 dBi reader antenna was fixed at a height of 2.5 m with a tilt of $\psi = 30°$, the TAG attached on a person's chest at the height of 1.25 m. The transmitted power was P_t = 35.4 dBm. All values were measured both at the axis of the identification area and for several off-axis offset p values.

a) b) c)

Fig. 20. Photograph of test configurations: a) a person with a chest-fixed TAG in an open area, b) a person with a chest-fixed TAG in a 4 m wide corridor, c) detail of the tag antenna

Fig.21 shows the simulated (2-ray model) and measured P_{rTAG} values as a function of the distance d from the reader in an open area. The plots show a very good agreement between the simulated and measured values, especially in the most important 2 - 8 m range. The maximum identification distance is approx. 9 m on axis, both the P_{rTAG} and $P_{rREADER}$ indicate the difficulties with the reliability of the off-axis identification. For practical implementations, the employment of more suitable reader antennas described in [23] can be recommended.

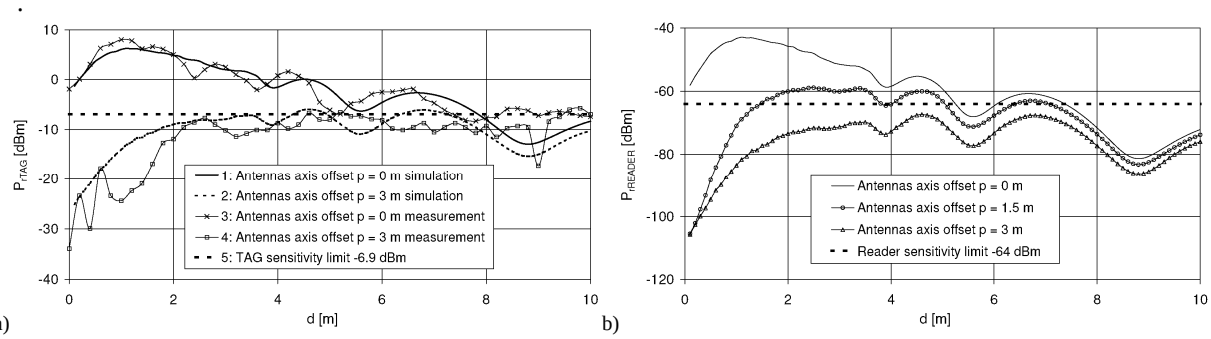

a) b)

Fig. 21 Simulated and measured received power P_{rTAG} (a) and $P_{rReader}$ (b) versus ground plane distance d from the reader antenna in an open area.

Figures 22 to 24 show the simulated (ray-tracing) and measured values of P_{rTAG} and P_{rREADER} in 4 m and 2 m wide corridors. The agreement is acceptable. The majority of differences can be explained by the estimated parameters of walls only, their non-homogenities and reflections from the metal door and window frames which were not included in the model.

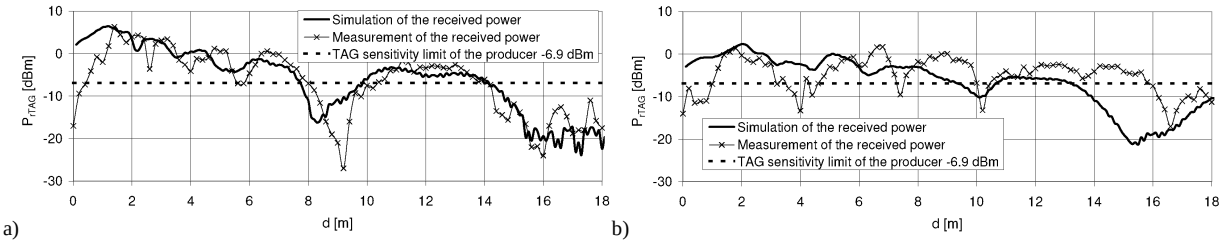

Fig. 22 Simulated and measured received power P_{rTAG} versus ground plane distance from the reader antenna in a 4 m wide corridor. (a) Antennas axis offset p = 0 m (b) Antennas axis offset p = 1.8 m.

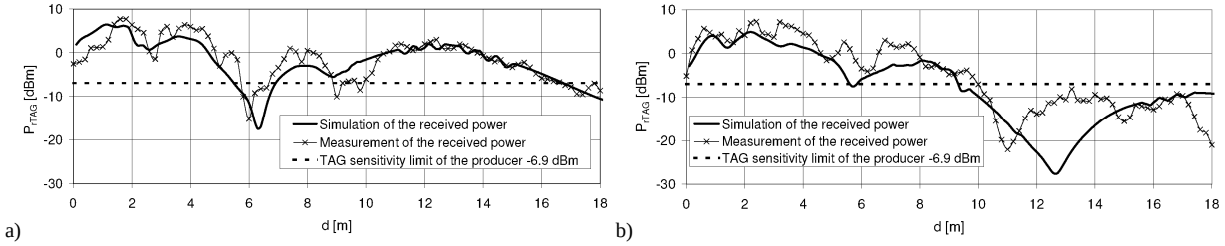

Fig. 23 Simulated and measured received power P_{rTAG} versus ground plane distance from the reader antenna in a 2 m wide corridor. (a) Antennas axis offset p = 0 m (b) Antennas axis offset p = 0.8 m.

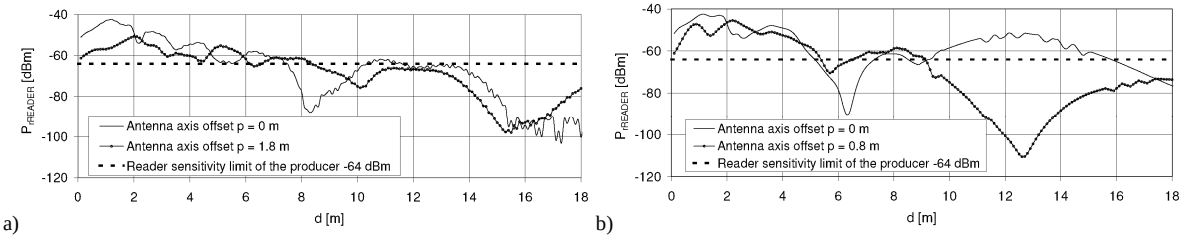

Fig. 24 Simulated received power P_{rREADER} versus ground plane distance from the reader antenna in 4 m (a) and 2 m (b) wide corridors.

Nevertheless, it was observed, that these influences had no essential impact on the identification distance of the RFID system. The measured $d_{\max}$ values are presented in Table 5.

Test configuration	Reader and tag antenna offset (m)	Read range (m)			
		Prediction			Ident. test
		Reader-tag sim.	Reader-tag meas.	Tag-reader sim.	d_{max} (m)
Open area	0	8.0	7.2	7.2	9
	1	7.7	6.2	7.0	6.5
	2	7.6	4.0	5.0	4
	3	7 *)	-	-	-
Corridor 4 m	0	13.8	13.8	11.0	9
	1.8	13	15.8	8.2	8
Corridor 2 m	0	16.4	16.4	15.8	16
	0.8	9.3	9.8	9.0	9

*) small margin of 0.8 dB over chip sensitivity does not allow the reliable RFID system performance

Tab. 5 Prediction and test of the read range of dual-loop patch array transponder in open area and corridors.

2.10 Summary of radio identification of people in UHF band

A reliable radio identification of people in moderate distances of a few meters should be based on an electromagnetic wave propagation mechanism. Due to the acceptable antenna dimensions for wearable purposes, UHF or microwave operational frequencies are supposed to be applied. Indeed, at these frequencies, the propagation of electromagnetic waves is influenced by several physical phenomena, namely by interferences, shadowing or waveguide effects. All of these effects can result in a false or even no identification. Besides, the functionality of the transponder antennas can be affected by the presence of a nearby human body that is able to detune the definite antenna structures and absorb a substantial part of the radiated or received power. Thus, the suitable tag antennas immune against the influence of a nearby human body have to be used. In order to guarantee the reliable identification, the whole UHF RFID system has to be tuned to ensure the sufficient power margins in both, the reader-TAG and TAG-reader signal paths.

References

[1] Finkenzeller, K., *RFID Handbook: Fundamentals and Applications in Contactless Smart Cards and Identification*, 2nd edition, John Wiley & Sons, 2005.

[2] Svanda, M., Polivka, M., Hudec, P., Application of the UHF RFID System for the Identification of Sportsmen in Mass Races. *In Proceedings of the European Microwave Association*. Pisa: Edizioni Plus - Universita di Pisa, Dec. 2007, Vol. 3, Issue 4.

[3] Polívka, M., Švanda, M., Hudec, P., Zvánovec, S., UHF RF Identification of People in Indoor and Open Areas. *IEEE Transactions on Microwave Theory and Techniques*. 2009, vol. 57, no. 5, p. 1341-1347.

[4] Gautherie, M. *Biological Basis of Oncologic Thermotherapy*, Springer-Verlag, Conference, Berlin, 1990.

[5] Foster, P. R. & Burberry, R,. A., Antenna problems in RFID systems, *Proceedings of IEE Colloquium RFID Technology*, pp. 31-35, London, UK, October 1999.

[6] Raumonen, P., et al., Folded dipole antenna near metal plate, *Proceedings of IEEE Antennas and Propagation Society International Symposium 2003*, pp. 848-851, ISBN 0-7803-7846-6, June 2003.

[7] Dobkin, D. M., Weigand, S. M., Environmental effects on RFID TAG antennas, *Proceedings of IEEE Antennas and Propagation Society International Symposium 2005*, ISBN 0-7803-8845-3, Washington, USA, July 2005.

[8] Griffin, J. D.; Durgin, G. D.; Haldi,A., Kippelen, B., RF TAG antenna performance on various materials using radio link budgets. *IEEE Antennas and Wireless Propagation Letters*, 2006, Vol. 5, pp. 247-250.

[9] Ukkonen, L.; Engles, D., Sydanheimo, L., Kivikoski, M., Planar wire-type inverted-F RFID TAG antenna mountable on metallic objects, *Proceeding of IEEE Antennas and Propagation Society International Symposium 2004*, pp. 101-104, Monterey, California, June 2004.

[10] Ukkonen, L.; Sydänheimo, L., Kivikoski, P. R., Effects of metallic plate size on the performance of microstrip patch-type TAG antennas for passive RFID. *IEEE Antennas and Wireless Propagation Letters*, Vol. 4, 2005, pp. 410 – 413, ISSN 1536 –1225

[11] Marrocco G.: RFID Antennas for the UHF Remote Monitoring of Human Subjects, *IEEE Transaction on Antennas and Propagation*, 2007, Vol. 55, No. 6.

[12] Conway G. A., Scanlon W. G.: Low-Profile Patch Antennas for Over-Body-Surface Communication at 2.45 GHz, 2007.

[13] Polivka, M., Svanda, M., Cerny, P., The Design of the Multiple-Arm Folded Dipole Antenna Operating Closely Spaced to a PEC. *Int. Journal on Wireless and Optical Communication*. 2008, vol. 2008, no. 5, p. 77-84.

[14] Svanda, M., Polivka, M., Horizontal Five-arm Folded Dipole over Metal Screening plane for UHF RFID of Dielectric Objects. *Microwave and Optical Technology Letters*. 2010, vol. 52, no. 10, p. 2291-2294.

[15] Lee, K. F., Chen, W., *Advances in Microstrip and Printed Antennas*, New York, John Wiley Sons, 1997

[16] Svanda M., Polivka M., Novel Dual-loop antenna Placed over Patch Array Surface for UHF RFID of Dielectric and Metallic Objects. *Microwave and Optical Technology Letters*. 2009, vol. 51, no. 3, p. 709-713.

[17] Svanda M., Polivka M., Two Novel Extremely Low-Profile Slot-Coupled Two-Element Patch Antennas for UHF RFID of People. *Microwave and Optical Technology Letters*. 2010, vol. 52, no. 2, p. 249-252.

[18] Troley Ponder RFID system. [Online], available at http://trolleyscan.com, 5.6.2006.

[19] Digital Mobile Radio towards Future Generation Systems. COST 231 Final Report, Brussels, 1996.

[20] Catedra, M.F., Perez-Arriaga, J., *Cell Planning for Wireless Communications*, Artech House, London, 1999.

[21] Pechac, P., Klepal, M., Novotny, K., Novel Approach to Indoor Propagation Modeling, *Radioengineering*, 2000, Vol. 9, No. 3, pp. 12-16.

[22] WinProp. [Online], available at http://www.awe-communications.com, 15.11.2008.

[23] Polivka, M., Holub, A., Mazanek, M., Collinear Microstrip Patch Antenna. *Radioengineering*, 2005, Vol. 14, No. 4, 2005, p. 40-42.

Ing. Milan Polívka, Ph.D. - CV

Affiliation: Czech Technical University in Prague, Faculty of Electrical Engineering, Department of Electromagnetic Field

Born: December 11, 1971, in Prague

Email: polivka@fel.cvut.cz

Education

2003 Ph.D., CTU in Prague, FEE

1996 M.S. (Ing.), CTU in Prague, FEE

Current position

Assistant professor at CTU in Prague, FEE, Dept. of Electromagnetic Field

Teaching activity

Antenna design and construction (17NKA), Computer modelling of fields (17PMP), CAD for microwave technique (17CAM)

Research area

General focus: antennas and microwave technique. Specialization: planar and small antennas, RFID transponder antennas, RFID of people.

Grant projects

2013	FRVŠ 1380 Aa „Laboratory development for education of solar systems, electrochemical sources and microwave measurement”
2008 – 2010	GAČR 102/08/1282 „Artificial electromagnetic structures for miniaturization of high-frequency and microwave radiation and circuit elements”
2009	FRVŠ 2359 F1a „Interactive stereoscopic imaging of electromagnetic fields”
2004 – 2006	GAČR 102/04/P131 „Multiband planar antennas with compact-shaped radiators”
2004	FRVŠ 2020 F1a „Assembly antenna design samples for subject 17NKA”
2002 – 2003	Detection system for localization of mobile phones in 13 prisons of the Czech Republic, design of antenna system
1997 – 2000	MŠMT VS97035 "Antenna laboratory“

Scientific publications and industrial property protection

10 IF journal papers, more than 70 conference papers, 2 chapters in foreign book, 5 patents, 7 utility models

Professional voluntary work

2011 – 2012	associate editor, Radioengineering journal
2010 – 2011	IEEE Czechoslovakia section, chairman
2010	IEEE Region 8 VCF Coordinator
2007 - 2009	IEEE Czechoslovakia MTT/AP/ED/EMC chapter, chairman
2007 – 2011	editoral board, Radioengineering journal

Reviewer: IEEE Transaction on Antennas and Propagation, IEEE Transactions on Microwave Theory and Technique, IEEE Antenna and Wireless Propagation Letters, IET Electronics Letters, Radioengineering